

Closed-Form EGN Model for FMF Systems

Original

Closed-Form EGN Model for FMF Systems / Amirabadi, M. A.; Kahaei, M. H.; Nezamalhoseini, S. A.; Arpanaei, F.; Carena, A.. - ELETTRONICO. - 2021:(2021). (Intervento presentato al convegno 2021 Asia Communications and Photonics Conference, ACP 2021 tenutosi a Shanghai, China nel 24-27 October 2021).

Availability:

This version is available at: 11583/2984820 since: 2024-01-17T08:18:13Z

Publisher:

Optica Publ.

Published

DOI:

Terms of use:

This article is made available under terms and conditions as specified in the corresponding bibliographic description in the repository

Publisher copyright

IEEE postprint/Author's Accepted Manuscript

©2021 IEEE. Personal use of this material is permitted. Permission from IEEE must be obtained for all other uses, in any current or future media, including reprinting/republishing this material for advertising or promotional purposes, creating new collecting works, for resale or lists, or reuse of any copyrighted component of this work in other works.

(Article begins on next page)

Closed-Form EGN Model for FMF Systems

M. A. Amirabadi*, M. H. Kahaei*, S. A. Nezamalhoseini*, F. Arpanaei⁺, and A. Carena⁺

*School of Electrical Engineering, Iran University of Science and Technology, Tehran-1684613114, Iran

⁺Politecnico di Torino, Dipartimento di Elettronica e Telecomunicazioni (DET), 10129 Torino, Italy.

m_amirabadi@elec.iust.ac.ir; {kahaei,nezam}@iust.ac.ir; {farhad.arpanaei, andrea.carena}@polito.it

Abstract: Recently, Enhanced Gaussian Noise (EGN) model of few-mode fiber nonlinearity has been proposed improving GN model accuracy. However, EGN is considerably complex. We propose a closed-form EGN model and provide substantial simulations indicating its accuracy. © 2021 The Author(s)

1. Introduction

The Gaussian Noise (GN) model of Few-Mode Fiber (FMF) nonlinear effects has been provided in [1] as a practical tool for estimating Nonlinear Interference Noise (NLIN) power in uncompensated FMF links. The GN model shows some errors in predicting NLIN power mostly due to the signal Gaussianity assumption [2]. Recently, GN model was extended in [3] and a complete Enhanced GN (EGN) model has been derived considering all NLIN components that improves the NLIN power prediction accuracy. Note that in this EGN model formulation, the carrier phase estimator is implicit in the model [3]. EGN model is computationally complex, which can make its extensive practical use difficult [2]. This paper proposes a closed-form EGN model from the integral-form EGN model presented in [3] and fully verifies it on a theoretical basis. Such approximation is effective in its present form especially for real-time quality of transmission evaluation.

2. Closed-form EGN model

Considering a rectangular Nyquist Wavelength Division Multiplexing (WDM) comb, and flat NLIN Power Spectral Density (PSD), the NLIN variance can be expressed as the multiplication of NLIN PSD and the bandwidth [4]. The PSD of p th mode and n th channel can be formulated by EGN model as in [2]

$$G_{EGN}^p(f_n) = G_{GN}^p(f_n) + G_{FON}^p(f_n) + G_{HON}^p(f_n), \quad (1)$$

where G_{GN} , G_{FON} , and G_{HON} are second, forth, and higher order noise contributions, respectively. Since Self Channel Interference (SCI) and Cross Channel Interference (XCI) are the dominant NLIN terms in dense WDM systems with large symbol rate, we only consider these terms. In other words, Multi Channel Interference (MCI) is not assumed in NLIN formulation [5]. Therefore, and by considering [3], the PSD of p th mode and n th channel can be expressed as

$$G_{EGN}^p(f_n) = \sum_{q=1}^D \left[3 \left(\underbrace{\kappa_1^{(n,q)^2} \kappa_1^{(n,p)} P_{n,q}^2 P_{n,p} E(n, p, n, q)}_{GN,SCI} + 2 \sum_{n' \neq n} \underbrace{\kappa_1^{(n',q)^2} \kappa_1^{(n,p)} P_{n',q}^2 P_{n,p} E(n, p, n', q)}_{GN,XCI} \right) + \left(\underbrace{\kappa_2^{(n,q)} \left(\kappa_1^{(n,p)} 5 P_{n,q}^2 P_{n,p} E(n, p, n, q) + \kappa_1^{(n,q)} P_{n,q} P_{n,p} P_{n,q} E(n, p, n, q) \right)}_{FON,SCI} \right. \right. \\ \left. \left. + 2 \sum_{n' \neq n} \underbrace{\kappa_2^{(n',q)} \left(\kappa_1^{(n,p)} 5 P_{n',q}^2 P_{n,p} E(n, p, n', q) + \kappa_1^{(n,q)} P_{n',q} P_{n',p} P_{n,q} E(n, p, n', q) \right)}_{FON,XCI} \right) + \left(\underbrace{\kappa_3^{(n,q)} P_{n,q}^2 P_{n,p} E(n, p, n, q)}_{HON,SCI} + 2 \sum_{n' \neq n} \underbrace{\kappa_3^{(n',q)} P_{n',q}^2 P_{n',p} E(n, p, n', q)}_{HON,XCI} \right) \right], \quad (2)$$

where D is number of modes, $P_{n,p}$ is the power of the n th channel of p th mode, $\kappa_1^{(n,p)} = \mu_2^{(n,p)}$, $\kappa_2^{(n,p)} = \mu_4^{(n,p)} - 2\mu_2^{(n,p)^2}$, and $\kappa_3^{(n,p)} = \mu_6^{(n,p)} - 4\mu_4^{(n,p)}\mu_2^{(n,p)} + 12\mu_2^{(n,p)^3}$, where $\mu_2^{(n,p)}$, $\mu_4^{(n,p)}$, and $\mu_6^{(n,p)}$ denote the second, fourth, and sixth order moment of the constellation of n th channel of p th mode, respectively. Moreover, the $E(n, p, n', q)$ term is equal to

$$E(n, p, n', q) = \frac{\tilde{\gamma}_{pq}^2}{4} \iint \left| \frac{1 - e^{-\alpha_p L_s} e^{j[\beta_q(f_1+f_2-f_n) - \beta_p(f_1) + \beta_p(f_n) - \beta_q(f_2)]L_s}}{\alpha_p - j[\beta_q(f_1+f_2-f_n) - \beta_p(f_1) + \beta_p(f_n) - \beta_q(f_2)]} \frac{1 - e^{j[\beta_q(f_1+f_2-f_n) - \beta_p(f_1) + \beta_p(f_n) - \beta_q(f_2)]N_s L_s}}{1 - e^{j[\beta_q(f_1+f_2-f_n) - \beta_p(f_1) + \beta_p(f_n) - \beta_q(f_2)]L_s}} \right|^2 df_1 df_2, \quad (3)$$

where α_p shows the attenuation, L_s is span length, N_s is number of spans, $\beta_p(f)$ is the propagation constant of p th mode, $\tilde{\gamma}_{pp} = \frac{8}{9}\gamma f_{pp}$, $\tilde{\gamma}_{pq} = \frac{4}{3}\gamma f_{pq}$ with γ being the Kerr nonlinearity coefficient, and $f_{pq} = \frac{A_{eff}}{I_p I_q} \iint F_p^2 F_q^2 dx dy$ representing the nonlinear coupling coefficient between the modes p and q where $F_p(x, y)$ is the spatial profile of p th mode, $I_p = \iint F_p^2(x, y) dx dy$, A_{eff} shows the effective area of the fundamental mode [6]. $f_1 \in [f_n - B_{ch,n}/2, f_n + B_{ch,n}/2]$ and $f_2 \in [f_{n'} - B_{ch,n'}/2, f_{n'} + B_{ch,n'}/2]$ with $B_{ch,n}$ and $B_{ch,n'}$ showing the bandwidths of the n th and n' th channels, respectively. We use the incoherency approximation, i.e.,

$(1 - e^{j|\beta_q(f_1+f_2-f_n)-\beta_p(f_1)+\beta_p(f_n)-\beta_q(f_2)|L_s}) / (1 - e^{j|\beta_q(f_1+f_2-f_n)-\beta_p(f_1)+\beta_p(f_n)-\beta_q(f_2)|L_s}) \rightarrow N_s$ [5]. Moreover, we can approximate the numerator term $|1 - e^{-\alpha_p L_s} e^{j|\beta_q(f_1+f_2-f_n)-\beta_p(f_1)+\beta_p(f_n)-\beta_q(f_2)|L_s}|^2 \approx (1 - e^{-\alpha_p L_s})^2$ [4]. Therefore, using $\beta_p(f) = 2\pi\beta_{1p}f + 2\pi^2\beta_{2p}f^2$, (3) can be approximated by

$$E(n, p, n', q) \approx N_s \frac{\tilde{\gamma}_{pq}^2}{4} \iint L_{eff}^2 \left[1 + L_{eff,a}^2 \left(2\pi(\beta_{1q} - \beta_{1p})(f_2 - f_n) - 4\pi^2\beta_{2q}(f_1 - f_n)(f_2 - f_n) \right)^2 \right] df_1 df_2, \quad (4)$$

where β_{1p} is the inverse group velocity parameter of p th mode, and $\beta_{2p} = |D_p|c/(2\pi v^2)$, D_p is the dispersion coefficient of p th mode, v is the center frequency of the WDM comb, c is the light speed, $L_{eff} = (1 - e^{-\alpha_p L_s})/\alpha_p$, and $L_{eff,a} = 1/\alpha_p$. By noting that $\int \rho/(1 + \rho^2 x^2) dx = \tan^{-1}(\rho x)$, $Ti_2(\rho x) = \int_0^x \tan^{-1}(\rho y)/(\rho y) dy$ [7], and $Ti_2(x) \approx \pi/2 \ln(x/2 + \sqrt{(x/2)^2 + 1})$ [7], (4) can be expressed as

$$E(n, p, n', q) \approx N_s \frac{\tilde{\gamma}_{pq}^2}{4} \frac{L_{eff}^2}{4\pi\beta_{2q}L_{eff,a}} \left[\ln \left(\pi^2\beta_{2q}L_{eff,a}B_{chn} \left(\frac{\beta_{1q} - \beta_{1p}}{2\pi\beta_{2q}} + f_n - f_{n'} + \frac{B_{chn'}}{2} \right) + \sqrt{\left(\pi^2\beta_{2q}L_{eff,a}B_{chn} \left(\frac{\beta_{1q} - \beta_{1p}}{2\pi\beta_{2q}} + f_n - f_{n'} + \frac{B_{chn'}}{2} \right) \right)^2 + 1} \right) + \ln \left(\pi^2\beta_{2q}L_{eff,a}B_{chn} \left(f_{n'} - \frac{\beta_{1q} - \beta_{1p}}{2\pi\beta_{2q}} - f_n + \frac{B_{chn'}}{2} \right) + \sqrt{\left(\pi^2\beta_{2q}L_{eff,a}B_{chn} \left(f_{n'} - \frac{\beta_{1q} - \beta_{1p}}{2\pi\beta_{2q}} - f_n + \frac{B_{chn'}}{2} \right) \right)^2 + 1} \right) \right]. \quad (5)$$

By substituting the obtained $E(n, p, n', q)$ approximation in (2), the PSD of the nonlinear noise of the n th channel of the p th mode can be obtained. However, we show in simulation results that this formulation underestimates the NLIN PSD. The FON terms have negative coefficient and removing them leads to NLIN PSD overestimation. We depict in our experiments that neglecting the FON term, $P_{n',q}P_{n',p}P_{n,q}E(n, p, n', q)$, can properly compensate this underestimation. Therefore, the PSD of p th mode and n th channel can be formulated by

$$G_{EGN}^p(f_n) = \sum_{q=1}^D \left[3 \left(\kappa_1^{(n,q)^2} \kappa_1^{(n,p)} P_{n,q}^2 P_{n,p} E(n, p, n, q) + 2 \sum_{n' \neq n} \kappa_1^{(n',q)^2} \kappa_1^{(n,p)} P_{n',q}^2 P_{n,p} E(n, p, n', q) \right) + \left(\kappa_2^{(n,q)} \kappa_1^{(n,p)} 5P_{n,q}^2 P_{n,p} E(n, p, n, q) + 2 \sum_{n' \neq n} \kappa_2^{(n',q)} \kappa_1^{(n,p)} 5P_{n',q}^2 P_{n,p} E(n, p, n', q) \right) + \left(\kappa_3^{(n,q)} P_{n,q}^2 P_{n,p} E(n, p, n, q) + 2 \sum_{n' \neq n} \kappa_3^{(n',q)} P_{n',q}^2 P_{n,p} E(n, p, n', q) \right) \right]. \quad (6)$$

3. Simulation results

In this section, the accuracy of proposed closed-form EGN model versus integral-form full EGN model presented in [3] is substantially investigated. The Generalized Signal to Noise Ratio (GSNR) is considered which contains the effect of NLIN and amplified spontaneous emission. The following FMF link parameters are used; the modulation format is PM-QPSK with the symbol rate 64 GBaud and the channel spacing 75 GHz. 10 spans are considered each with 100 km length. 3 modes, each with 66 channels with the center frequency 1550 nm are used. The values for nonlinear coupling coefficient, dispersion coefficient, inverse group velocity, and attenuation are taken from [6]. At each span, an erbium doped fiber amplifier with 5 dB noise figure compensates FMF attenuation. All Figs plot GSNR of central channel of LP01 or LP11a/b mode. The link-state is full-load with the same modulation format for different channels and modes.

Figs. 1a and 1b investigate the effect of considering $P_{n',q}P_{n',p}P_{n,q}E(n, p, n', q)$ term in (6) for LP01 and LP11a/b modes, respectively. As seen, considering (6) with $P_{n',q}P_{n',p}P_{n,q}E(n, p, n', q)$ term underestimates the NLIN power, and removing this term results in better accuracy. The accuracy of closed-form EGN model for different modulation formats is indicated by GSNR plots in Figs. 1c and 1d where the optimum launched power is deployed for different channels and modes. The GSNR difference of closed-form and integral-form EGN model is always below 0.4 dB. Fig. 2 plots GSNR versus launched power per channel-mode for closed-form and integral-form EGN

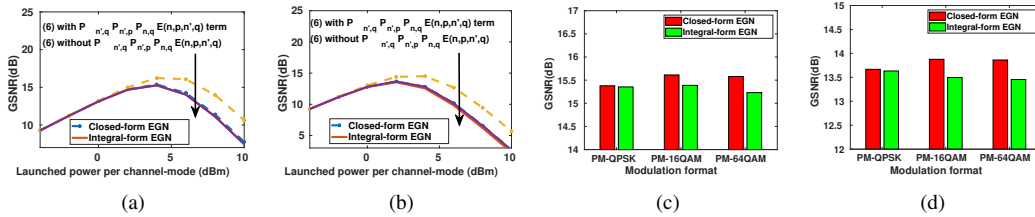


Fig. 1: GSNR versus launched power per channel-mode for closed-form and integral-form EGN model, considering (6) with/without $P_{n',q}P_{n',p}P_{n,q}E(n, p, n', q)$ term for a) LP01 and b) LP11a/b modes; and GSNR of the optimum launched power per channel-mode versus modulation format for closed-form and integral-form EGN model, for c) LP01 and d) LP11a/b modes.

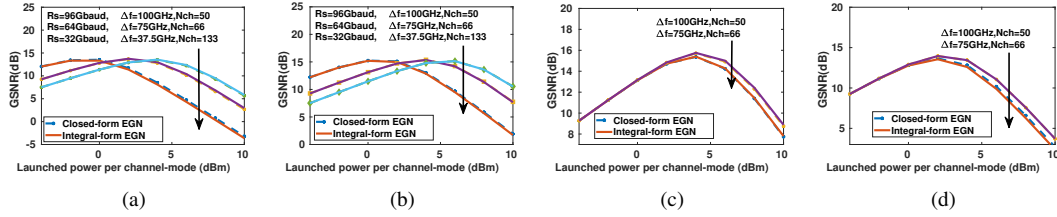


Fig. 2: GSNR versus launched power per channel-mode for closed-form and integral-form EGN model, considering different baudrates-channel spacing for a) LP01 and b) LP11a/b modes; and considering different channel spacing for c) LP01 and d) LP11a/b modes.

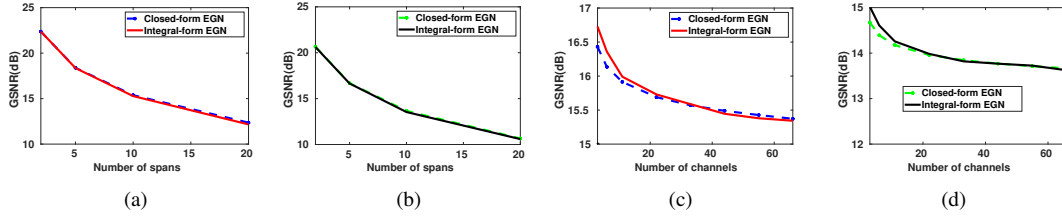


Fig. 3: GSNR versus number of spans, for closed-form and integral-form EGN model, considering the optimum launched power per channel-mode for a) LP01 and b) LP11a/b modes; and GSNR versus number of channels, for closed-form and integral-form EGN model, considering the optimum launched power per channel-mode considering full-load link-state for c) LP01 and d) LP11a/b modes.

model, considering different baudrates-channel spacing (Figs. 2a and 2b) and different channel spacing (Figs. 2c and 2d). It is indicated that closed-form EGN model is quite effective while considering different baudrates and channel spacing in both LP01 and LP11a/b modes. Figs. 3a and 3b show good convergence of closed-form EGN model towards the integral-form EGN model curve considering different number of spans for both LP01 and LP11a/b modes. Figs. 3c and 3d indicate that closed-form EGN model is accurate for sufficiently large number of channels for both LP01 and LP11a/b modes.

4. Conclusion

In this paper, we presented a closed-form EGN model for FMF systems. Substantial simulations indicated the proposed formulation to be accurate for sufficiently large number of channels. The GSNR difference compared with integral-form EGN model is always below 0.4 dB.

Acknowledgement

This work was supported by the Italian Ministry for University and Research (PRIN 2017, project FIRST).

References

1. G. Rademacher et al. “Nonlinear Gaussian noise model for multimode fibers with space-division multiplexing”, *Journal of Lightwave Technology*, Vol. 34, No. 9, pp. 2280-2287, 2016.
2. P. Poggiolini et al. “A simple and effective closed-form GN model correction formula accounting for signal non-Gaussian distribution”, *Journal of Lightwave Technology*, Vol. 33, No. 2, pp. 459-473, 2015
3. M. A. Amirabadi et al. “Joint Power and Gain Allocation in MDM-WDM Optical Communication Networks Based on Extended Gaussian Noise Model”, arXiv preprint arXiv:2107.08602, 2021.
4. P. Poggiolini, “The GN model of non-linear propagation in uncompensated coherent optical systems”, *Journal of Lightwave Technology*, Vol. 30, No. 24, pp. 3857–3879, 2012.
5. P. Poggiolini et al. “Analytical and experimental results on system maximum reach increase through symbol rate optimization”, *Journal of Lightwave Technology*, Vol. 34, No. 8, pp. 1872–1885, 2016.
6. S. Mumtaz et al. “Nonlinear Propagation in Multimode and Multicore Fibers: Generalization of the Manakov Equations”, *Journal of Lightwave Technology*, Vol. 31, No. 3, pp. 398-406, 2012.
7. C. I. Vălean, *(Almost) impossible integrals, sums, and series*, Springer, 2019.